JACC: CARDIOVASCULAR IMAGING VOL. 13, NO. 11, 2020

PUBLISHED BY ELSEVIER

ORIGINAL RESEARCH

Defining Myocardial Abnormalities Across the Stages of Chronic Kidney Disease

A Cardiac Magnetic Resonance Imaging Study

Manvir K. Hayer, MBChB,[a,b] Ashwin Radhakrishnan, BMBS,[a,c] Anna M. Price, MBChB,[a,b] Boyang Liu, MBBS,[a,c] Shanat Baig, MBBS,[a,c] Christopher J. Weston, PhD,[d,e] Luca Biasiolli, DPhil,[f] Charles J. Ferro, MD,[a,b] Jonathan N. Townend, MD,[a,c] Richard P. Steeds, MD,[a,c] Nicola C. Edwards, PhD,[a,g] on behalf of the Birmingham Cardio-Renal Group*

ABSTRACT

OBJECTIVES A proof of concept cross-sectional study investigating changes in myocardial abnormalities across stages of chronic kidney disease (CKD). Characterizing noninvasive markers of myocardial fibrosis on cardiac magnetic resonance, echocardiography, and correlating with biomarkers of fibrosis, myocardial injury, and functional correlates including exercise tolerance.

BACKGROUND CKD is associated with an increased risk of cardiovascular death. Much of the excess mortality is attributed to uremic cardiomyopathy, defined by increased left ventricular hypertrophy, myocardial dysfunction, and fibrosis. The prevalence of these abnormalities across stages of CKD and their impact on cardiovascular performance is unknown.

METHODS A total of 134 nondiabetic, pre-dialysis subjects with CKD stages 2 to 5 without myocardial ischemia underwent cardiac magnetic resonance (1.5-T) including; T_1 mapping (biomarker of diffuse fibrosis), T_2 mapping (edema), late gadolinium enhancement, and assessment of aortic distensibility. Serum biomarkers including collagen turnover (P1NP, P3NP), troponin T, and N-terminal pro-B-type natriuretic peptide were measured. Cardiovascular performance was quantified by bicycle cardiopulmonary exercise testing and echocardiography.

RESULTS Native myocardial T_1 times increased incrementally from stage 2 to 5 (966 ± 21 ms vs. 994 ± 33 ms; $p < 0.001$), independent of hypertension and aortic distensibility. Left atrial volume, E/e′, N-terminal pro-B-type natriuretic peptide, P1NP, and P3NP increased with CKD stage ($p < 0.05$), while effort tolerance (% predicted VO_2Peak, %VO_2VT) decreased ($p < 0.001$). In multivariable linear regression models, estimated glomerular filtration rate was the strongest predictor of native myocardial T_1 time ($p < 0.001$). Native myocardial T_1 time, left atrial dilatation, and high-sensitivity troponin T were independent predictors of % predicted VO_2Peak ($p < 0.001$).

CONCLUSIONS Imaging and serum biomarkers of myocardial fibrosis increase with advancing CKD independent of effects of left ventricular afterload and might be a key intermediary in the development of uremic cardiomyopathy. Further studies are needed to determine whether these changes lead to the increased rates of heart failure and death in CKD. (Left Ventricular Fibrosis in Chronic Kidney Disease [FibroCKD]; NCT03176862)
(J Am Coll Cardiol Img 2020;13:2357–67) © 2020 by the American College of Cardiology Foundation.

From the [a]Institute of Cardiovascular Science, University of Birmingham, Birmingham, United Kingdom; [b]Department of Nephrology, Queen Elizabeth Hospital, Birmingham, United Kingdom; [c]Department of Cardiology, Queen Elizabeth Hospital, Birmingham, United Kingdom; [d]NIHR Birmingham Biomedical Research Centre, University Hospitals Birmingham NHS Foundation Trust and University of Birmingham, Birmingham, United Kingdom; [e]Institute of Immunology and Immunotherapy, University of Birmingham, Birmingham, United Kingdom; [f]Oxford Centre for Clinical Magnetic Resonance Research (OCMR), Radcliffe Department of Medicine, University of Oxford, Oxford, United Kingdom; and the [g]Green Lane Cardiovascular Service, Auckland, New Zealand. *Details about the Birmingham Cardio-Renal Group can be found at https://www.birmingham.ac.uk/research/activity/cardiovascular-sciences/research.

ISSN 1936-878X/$36.00 https://doi.org/10.1016/j.jcmg.2020.04.021

ABBREVIATIONS AND ACRONYMS

CKD = chronic kidney disease

CMR = cardiac magnetic resonance

CPESE = cardiopulmonary exercise testing with stress echocardiography

GLS = global longitudinal strain

LGE = late gadolinium enhancement

P1NP = pro-collagen N-terminal type 1 peptide

P3NP = pro-collagen N-terminal type 3 peptide

VO_2Peak = peak oxygen carrying capacity

%VO_2VT = percent predicted peak oxygen carrying capacity at the ventilatory threshold

Chronic kidney disease (CKD) is a major risk factor for cardiovascular (CV) disease with a graded, inverse relationship between CV risk and glomerular filtration rate (GFR) independent of age, sex, and other risk factors (1). The major health care burden of CKD relates to patients with early-stage disease in whom CV risk usually outweighs the risk of progression to end stage renal disease (ESRD) (2). CV disease associated with CKD is complex. Although the prevalence of coronary artery disease (CAD) is increased, most deaths in late-stage CKD are due to sudden cardiac death and heart failure and are thought to be a result of heart muscle disease, frequently termed uremic cardiomyopathy (3).

Recently, imaging studies using echocardiography and cardiac magnetic resonance (CMR) have redefined uremic cardiomyopathy in CKD as a distinct phenotype consisting of prognostically significant changes including left ventricular (LV) hypertrophy, left atrial (LA) dilatation, diastolic dysfunction, and reduced myocardial deformation—a surrogate of myocardial fibrosis (4-6). The application of CMR native T_1 mapping techniques, a biomarker of interstitial fibrosis, demonstrated increased T_1 times in ESRD with associations between elevated T_1 times and serum markers of fibrosis, myocardial strain, and levels of serum troponin (7,8). Increased native myocardial T_1 times are also increased in patients with early-stage CKD compared with hypertensive and healthy control subjects (9). However, the pathophysiological and functional significance of increased interstitial fibrosis in CKD is not yet clear. The aim of this cross-sectional proof of concept study was to investigate myocardial changes in CKD stages 2 to 5. Associations were sought between native myocardial T_1 values and indexes of exercise tolerance, ventricular deformation, serum concentrations of biomarkers of fibrosis, and bone mineral metabolism, which have all been implicated in the development of uremic cardiomyopathy.

METHODS

Pre-dialysis patients with CKD stages 2 to 5 (estimated glomerular filtration rate [eGFR] ≤90 to ≥15 ml/min/1.73 m^2) were recruited from renal clinics in Birmingham, United Kingdom, between August 2015 and May 2018. Pre-screening of clinics was performed ensuring inclusion/exclusion criteria. Patient information sheets were posted in advance, and patients were approached and formally screened at their clinic appointment. Recruitment was stratified by CKD stage (4-variable Modification of Diet in Renal Disease formula). Exclusion criteria were: diabetes mellitus, known coronary artery disease (angina, myocardial infarction, prior percutaneous or surgical revascularization, evidence of myocardial ischemia on noninvasive testing), heart failure, moderate or severe valvular heart disease, stroke, or peripheral vascular disease. Myocardial ischemia was excluded in all cases using either exercise stress echocardiography with LV opacification (Sonovue, Bracco, Milano, Italy) or 99m technetium-tetrofosmin single-photon emission computed tomography with computed tomography attenuation (Symbia T16, Siemens, Erlangen, Germany). The study was approved by the National Research Ethics Service-East Midlands (15/EM/0280). Patient participation was voluntary, and all subjects gave written informed consent.

Demographic, medical comorbidities, blood, and proteinuria data were collected. Subjects underwent assessment as follows.

CARDIAC MAGNETIC RESONANCE. All studies were performed at 1.5-T (Siemens Avanto, Erlangen, Germany). Standard protocols for LV function and mass were performed using steady-state free precession imaging (10). Myocardial characterization was assessed using T_1 mapping, T_2 mapping, and inversion recovery imaging after gadolinium (if eGFR ≥30 ml/min/1.73 m^2). An ECG-gated Modified Look-Locker Inversion recovery sequence with a 3(3) 3(3)5 heartbeat sampling protocol (Siemens WIP 448) was performed pre-contrast (to assess native myocardial T_1) and post-contrast (for extracellular volume [ECV]) at basal and mid-short axis levels in diastole. Typical acquisition parameters were: pixel bandwidth 977 Hz/pixel; echo time = 1.1 ms; flip angle = 35°; matrix = 144 × 256 slice thickness 6 mm. T_2 mapping (T_2-prepared single-shot steady-state free precession technique) was performed at identical basal and mid short-axis levels as T_1 maps. Typical T_2 acquisition parameters: 3 single-shot images were

The authors attest they are in compliance with human studies committees and animal welfare regulations of the authors' institutions and Food and Drug Administration guidelines, including patient consent where appropriate. For more information, visit the *JACC: Cardiovascular Imaging* author instructions page.

Manuscript received December 9, 2019; revised manuscript received March 30, 2020, accepted April 17, 2020.

acquired at different T_2-preparation times (0, 24, and 55 ms, respectively), ECG triggered, TE = 1.12 ms, flip angle = 70°, voxel size 2.2 × 1.8 × 6.0 mm, slice thickness 6 mm. Motion correction and fitting were performed to estimate coefficients of the decay function, which were then used to estimate T_2 times. Standard inversion recovery imaging was performed 7 to 10 min after gadolinium-based contrast agent (Gadovist 0.15 mmol/kg, Bayer, Whippany, New Jersey) for assessment of late gadolinium enhancement (LGE).

OFFLINE ANALYSIS. Analysis of LV function, volume, and mass was performed with delineation of papillary muscles and trabeculations using thresholding (CVi 42, version 5.3.4, Circle Vascular Imaging, Calgary, Alberta, Canada) as previously described (10). Tissue tracking for 2-dimensional myocardial global longitudinal strain (GLS) and global circumferential strain was performed using standard views and indexed for LV end-diastolic volume as previously described (11). T_1 and T_2 times were measured from the parametric maps with endocardial and epicardial borders delineated and a 20% offset was used to avoid blood pool contamination. Anterior and inferior septal borders were defined with semiautomated segmentation of the LV in accordance with the American Heart Association 17-segment model. Septal T_1 time (average of anteroseptal and inferoseptal segments) was reported, avoiding measurement in any region with LGE. ECV and indexed ECV (ECV fraction × LV end-diastolic myocardial volume normalized to the body surface area) was calculated using validated formulas as previously described (10). Intraobserver and interobserver variability for T_1 were assessed using data from 30 anonymized subjects, randomly assessed from the cohort and analyzed by observers' blind to all clinical data. A T_1 mapping and ECV standardization phantom was scanned fortnightly during the study period to ensure stability of measurements (12).

AORTIC DISTENSIBILITY. A breath held retrospective ECG-gated axial steady-state free precession cine of the ascending aorta at the level of the pulmonary artery was acquired. Typical acquisition parameters were TE = 1.2 ms, TR = 56.8 ms, flip angle = 61°, voxel size = 1.8 × 1.4 × 6 mm^3, number of cine images = 1. Aortic lumen was detected and segmented automatically using a dedicated analysis tool developed in Matlab (Mathworks, Natick, Massachusetts). The maximal and minimal cross-sectional lumen area (mm^2) were measured as the average from 3 systolic (A_{max}) and 3 diastolic (A_{min}) images in the ascending aorta to calculate the change in aortic lumen area $(A_{max} - A_{min})/A_{min}$. Aortic distensibility was obtained dividing the aortic area change by the pulse pressure measured as the average of 3 non-invasive blood pressure readings taken at the time of cine acquisition.

CARDIOPULMONARY EXERCISE TESTING WITH STRESS ECHOCARDIOGRAPHY. A maximal bicycle ergometer cardiopulmonary exercise stress echocardiogram (cardiopulmonary exercise testing with stress echocardiography [CPESE], GE Case ES V6.61) was performed using an individualized Ramp protocol based on sex, age, and weight (13). Ventilatory gases were analyzed breath-by-breath and averaged over 10-s intervals. Subjects exercised until exhaustion. A respiratory exchange ratio ≥1.1 and % predicted heart rate ≥85% were used as markers of adequate effort tolerance. Ventilatory threshold (VT) was defined as the point of intersection between the line of departure of VO_2 from the line of identity drawn through a plot of VCO_2 versus VO_2 (the v-slope method) (14). Parameters of exercise tolerance included; % predicted peak oxygen carrying capacity (VO_2Peak) and % predicted peak oxygen capacity at the ventilatory threshold (% predicted VO_2VT).

Systolic function (ejection fraction, myocardial strain), diastolic function (LA volume index, ratio transmitral E-wave/lateral myocardial TDI e′ wave; E/e′), and evidence of myocardial ischemia were assessed by rest and stress echocardiography (EPIQ, Phillips, Eindhoven, the Netherlands). Myocardial strain values were indexed for LV volume to adjust for volume load. In subjects with myocardial ischemia excluded by single-photon emission computed tomography with computed tomography as a part of their kidney transplant work-up, only cardiopulmonary exercise test was performed.

BLOOD BIOMARKERS. Plasma and serum were tested for pro-collagen N-terminal type 1 peptide (P1NP) and pro-collagen N-terminal type 3 peptide (P3NP) using the Elecsys total P1NP kit (Roche Diagnostics, Mannheim, Germany) and the Orion UniQ P3NP RIA kit (Orion Diagnostica, Espoo, Finland), respectively. Plasma was also tested for human-FGF-23 (C-term, Immunotopics, San Clemente, California) and human alpha Klotho (IBL International, Hamburg, Germany) using enzyme-linked immunosorbent assays. N-terminal pro-B-type natriuretic peptide (NT proBNP) and troponin-T were measured using standard diagnostic assays (Roche Diagnostics, Indianapolis, Indiana).

TABLE 1 Patient Characteristics

	CKD Stage 2 (n = 38)	CKD Stage 3 (n = 37)	CKD Stage 4 (n = 32)	CKD Stage 5 (n = 30)	p Value
Age, yrs	52 ± 14	59 ± 13	55 ± 15	51 ± 16	0.754
Male	25 (66)	20 (54)	22 (69)	16 (53)	0.449
Ethnicity					0.295
Caucasian	29 (76)	31 (84)	22 (69)	21 (70)	
South Asian	3 (8)	4 (11)	9 (28)	5 (17)	
Afro Caribbean	5 (13)	2 (5)	1 (3)	3 (10)	
Other	1 (3)	0 (0)	0 (0)	1 (3)	
Smoker					0.222
Current	9 (24)	4 (11)	2 (6)	3 (10)	
Ex	10 (26)	7 (19)	7 (22)	10 (35)	
Never	19 (50)	26 (70)	23 (72)	17 (57)	
BMI, kg/m^2	27 ± 4	29 ± 4	28 ± 3	28 ± 4	0.125
Blood pressure, mm Hg	128 ± 17	132 ± 15	140 ± 16	139 ± 17	**<0.001**
Heart rate, beats/min	71 ± 12	76 ± 15	75 ± 13	79 ± 16	**0.036**
Etiology					**0.016**
Primary GN	14 (38)	8 (22)	8 (25)	5 (17)	
Vasculitis	10 (27)	6 (16)	4 (13)	3 (10)	
Cystic disease	7 (19)	15 (41)	7 (22)	6 (20)	
Other	6 (16)	8 (22)	13 (41)	16 (53)	
Drugs					
ACEi/ARB	27 (32)	31 (36)	21 (59)	7 (19)	**<0.001**
CCB	12 (21)	14 (25)	13 (23)	17 (30)	0.229
Beta-blocker	2 (9)	6 (27)	8 (36)	6 (27)	0.149
Diuretics	5 (20)	4 (16)	7 (28)	9 (36)	0.175
Statin	13 (31)	11 (26)	11 (26)	7 (17)	0.724
Hemoglobin, g/l	141 ± 13	132 ± 10	127 ± 14	114 ± 15	**<0.001**
eGFR, ml/min/1.73 m^2	67 (64–72)	41 (34–49)	21 (18–25)	10 (9–12)	**<0.001**
ACR, mg/mol	9 (3.0–56.3)	10.9 (2.7–20.9)	44.7 (13.8–107.7)	82.5 (26.6–154.1)	**<0.001**
Phosphate, mmol/l	1.10 (0.91–1.30)	1.07 (0.92–1.18)	1.26 (1.12–1.38)	1.52 (1.31–1.61)	**<0.001**
PTH, pmol/l	5.3 (3.5–7.2)	7.0 (5.6–11.8)	15.8 (10.8–21.3)	35.3 (18.4–45.9)	**<0.001**
NT-proBNP, ng/l	38 (17–85)	106 (59–233)	199 (114–326)	423 (220–660)	**<0.001**
Troponin, ng/l	6 (4–8)	9 (6–13)	12 (7–24)	19 (14–29)	**<0.001**
Renin, ng/l	46.5 (18.0–74.6)	34.6 (14.9–92.1)	33.7 (13.4–115.4)	25.5 (16.8–76.8)	0.575
Aldosterone, pmol/l	179 (132–494)	184 (108–279)	309 (141–505)	315 (179–628)	**0.030**
P3NP, ug/l	2.85 (2.40–3.55)	3.20 (2.70–3.95)	4.35 (3.95–5.65)	4.95 (4.10–5.70)	**<0.001**
P1NP, ug/l	50 (34–70)	43 (27–61)	96 (65–127)	135 (99–238)	**<0.001**
FGF-23, RU/ml	70 (50–99)	133 (86–190)	225 (144–252)	563 (235–1,153)	**<0.001**
Alpha-Klotho, pg/ml	503 (355–578)	423 (323–701)	408 (296–492)	417 (372–958)	0.429

Values are mean ± SD, n (%), or median (interquartile range). The Jonckheere Terpstra test was used to assess for trend in continuous variables across the CKD stages. The chi-square test was used to assess the difference in categorical variables across the CKD stages. A p value <0.05 **(bold)** was considered to be statistically significant.

ACEi = angiotensin-converting enzyme inhibitor; ACR = albumin to creatinine ratio; ARB = angiotensin receptor blocker; BMI = body mass index; CCB = calcium-channel antagonist/blocker; eGFR = estimated glomerular filtration rate; FGF-23 = fibroblast growth factor 23; GN = glomerulonephritis; NT-proBNP = N-terminal pro-B-type natriuretic peptide; P1NP = pro-collagen N-terminal type 1 peptide; P3NP = pro-collagen N-terminal type 3 peptide; PTH = parathyroid hormone.

SAMPLE SIZE JUSTIFICATION AND STATISTICAL ANALYSIS. Previous in-house T_1 data in subjects with CKD demonstrated a standard deviation of 30 to 35 ms, which is consistent with published data (9,15). A sample size of 33 subjects per stage of CKD (n = 132 total) was needed to provide 80% power to detect a minimal detectable difference between groups of 30 ms with an alpha value of <5%. With this sample size, treating eGFR as a continuous variable would yield 80% power to detect a correlation coefficient with T_1 of 0.24.

All data were analyzed using SPSS version 24 (SPSS Inc., Chicago, Illinois). Normality was assessed using the Shapiro-Wilk test. Parametric variables are shown as mean ± SD, with median (interquartile range) used for nonparametric data. The Jonckheere-Terpstra test was performed to assess for trend in continuous variables across CKD stages. Categorical variables were compared across stages using the chi-square test. Pearson's or Spearman's correlation coefficients were used for continuous parametric and nonparametric variables, respectively. Linear regression modeling

TABLE 2 Left Ventricular Structure and Function on CMR

	CKD Stage 2 (n = 37)	CKD Stage 3 (n = 37)	CKD Stage 4 (n = 31)	CKD Stage 5 (n = 29)	p Value (Trend)
LVEDVi, ml/m^2	61 ± 12	60 ± 9	62 ± 13	70 ± 20	0.071
LVESVi, ml/m^2	18 ± 6	17 ± 6	22 ± 19	22 ± 9	0.071
LVEF, %	71 ± 8	70 ± 7	70 ± 8	69 ± 7	0.391
LV mass I, g/m^2	65 ± 12	64 ± 12	66 ± 15	74 ± 19	0.140
LA vol I, ml/m^2	33 ± 12	37 ± 13	38 ± 12	43 ± 14	**0.006**
LGE, %*	13 (35)	16 (43)	–	–	0.521
GLSi, %/ml	0.17 ± 0.05	0.17 ± 0.05	0.17 ± 0.06	0.15 ± 0.05	0.128
GCSi, %/ml	0.17 ± 0.06	0.18 ± 0.05	0.18 ± 0.06	0.15 ± 0.05	0.162
Aortic distensibility, × 10^{-3} mm Hg^{-1}	2.49 (1.57–3.94)	2.66 (1.67–3.82)	2.13 (1.51–2.91)	1.72 (1.10–3.12)	0.074
Native septal T_1, ms	966 ± 21	975 ± 31	980 ± 28	994 ± 33	**<0.001**
Native blood pool T_1, ms	1,503 ± 92	1,528 ± 75	1,546 ± 93	1,578 ± 80	**0.001**
Post-contrast septal T_1, ms*	447 ± 30	430 ± 23	–	–	**0.023**
Post-contrast blood T_1, ms*	299 ± 29	279 ± 28	–	–	**0.011**
Septal ECV*	0.27 ± 0.03	0.27 ± 0.04	–	–	0.482
Indexed ECV, ml/m^2*†	16 ± 4	15 ± 6	–	–	0.141
Native septal T_2, ms	54 ± 4	55 ± 4	54 ± 3	57 ± 5	**0.033**

Values are mean ± SD, n (%), or median (interquartile range). The Jonckheere Terpstra test was used to assess for trend in continuous variables across the CKD stages. The chi-square test was used to assess to difference in categorical variables across the CKD stages. A p value <0.05 was considered to be statistically significant **(bold)**. *Based on the n = 67 who were administered gadolinium. Patterns; right ventricular insertion point 21 of 67, mid wall 8 of 67, and subendocardial 0 of 67. Indexed ECV is calculated as using the following equation: iECV ml/m^2 = (ECV% × indexed LV mass)/(1.05 × 100). †Independent samples Student's *t*-test was used to calculate this p value as there were only 2 variables of interest.

ECV = extracellular volume; GCSi = indexed global circumferential strain; GLSi = indexed global longitudinal strain; LA = left atrial; LV = left ventricular; LVEDV = left ventricular end-diastolic volume; LVEF = left ventricular ejection fraction; LVESV = left ventricular end-systolic volume.

was performed to assess for the effect of potential confounders. Initially, univariate linear regression models were produced for each factor and the residuals were interrogated to assess the goodness of fit. Logarithmic-transformation was applied to factors with a poor fit, and goodness of fit was reassessed before producing multivariate linear regression models. A variance inflation factor >5 was taken to represent collinearity. For the regression model with native myocardial T_1 as the dependent variable, only factors thought to be clinically relevant to the question being asked were entered into a multivariate model alongside aortic distensibility. For the model with exercise capacity as the dependent variable, factors of clinical interest and factors that were significant on univariate analysis ($p < 0.05$) were considered for inclusion into the multivariate model. A backward stepwise approach was then used to remove those factors that were not independently associated with exercise capacity. A p value of <0.05 was considered statistically significant.

RESULTS

PATIENT CHARACTERISTICS. In total, 139 subjects were recruited. Two subjects were excluded following positive stress tests for ischemia. Patient characteristics are detailed in Table 1. The leading causes of renal disease were primary glomerulonephritis and polycystic kidney disease. Blood pressure was well controlled across the cohort with 127 of 137 (93%) on antihypertensive medication. Blood pressure was higher in more severe kidney disease. There were also differences in hemoglobin, phosphate, parathyroid hormone, and proteinuria with worsening CKD stage (Table 1).

LV STRUCTURE AND FUNCTION ON CMR. CMR data was available for 134 subjects following exclusion of 3 patients for claustrophobia (Table 2). LV hypertrophy (defined by age and sex-matched normal range) was evident in 14 subjects (10%). Indexed LV volume and mass did not differ significantly across CKD stages, although mass was higher in CKD stage 5 (Central Illustration). Indexed LA volume increased with stage of CKD ($p = 0.006$). Neither indexed CMR myocardial strain nor aortic distensibility differed between CKD stages.

MYOCARDIAL TISSUE CHARACTERIZATION. Native T_1 times and ECV. There was a significant trend for native myocardial T_1 times to increase with advancing CKD stage (native T_1 $p < 0.001$) (Central Illustration, Figure 1) and a correlation with LV mass (native T_1 $r = 0.231$; $p = 0.008$). Gadolinium was administered to 67 of 74 eligible subjects (eGFR ≥30 ml/min/1.73 m^2). Post-contrast myocardial T_1 times decreased with worsening CKD (post contrast T_1 $p = 0.023$). Extracellular volume and extracellular volume index did not differ between CKD stages 2 and 3. No data was available for CKD stage 4 and 5 (Table 2).

CENTRAL ILLUSTRATION **A Conceptual Overview of Myocardial Abnormalities Across the Spectrum of Chronic Kidney Disease**

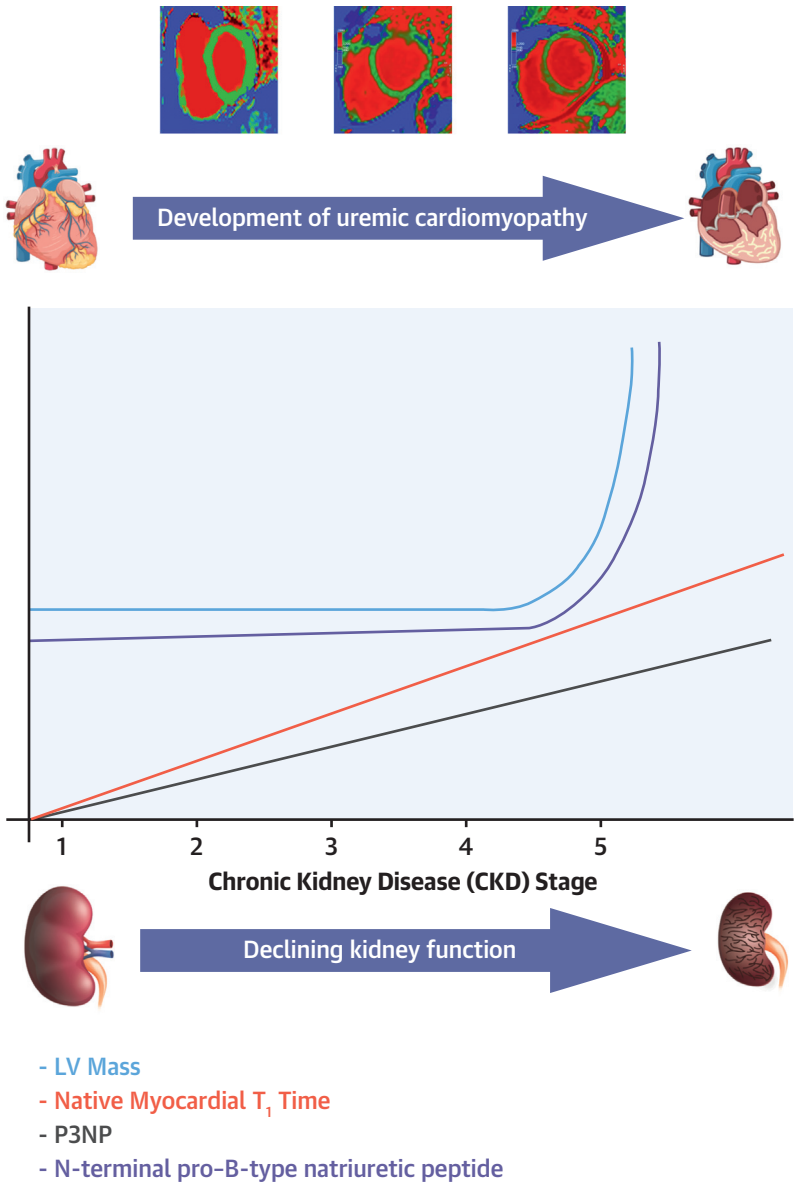

Hayer, M.K. et al. J Am Coll Cardiol Img. 2020;13(11):2357–67.

Native myocardial T_1 times increased with worsening stage of chronic kidney disease (CKD) and were accompanied by a rise in serum biomarkers of fibrosis and heart failure. Left ventricular (LV) mass only increased in severe CKD.

Native T_2 times. Myocardial T_2 times increased with progressive CKD severity (test for trend $p = 0.033$). On univariable analysis, myocardial T_2 time was correlated with native myocardial T_1 time ($r = 0.541$; $p < 0.001$).

Late gadolinium enhancement. LGE was present in 29 of 67 (43%) subjects with the patterns; right ventricular insertion point 21 of 67 (31%) and midwall/sub-epicardial 8 of 67 (12%). No patient had subendocardial LGE indicative of infarction. There was

FIGURE 1 Trend in Myocardial Native T_1 Times, LV Mass, Exercise and Echo-Based Global Longitudinal Strain Across the Stages of CKD

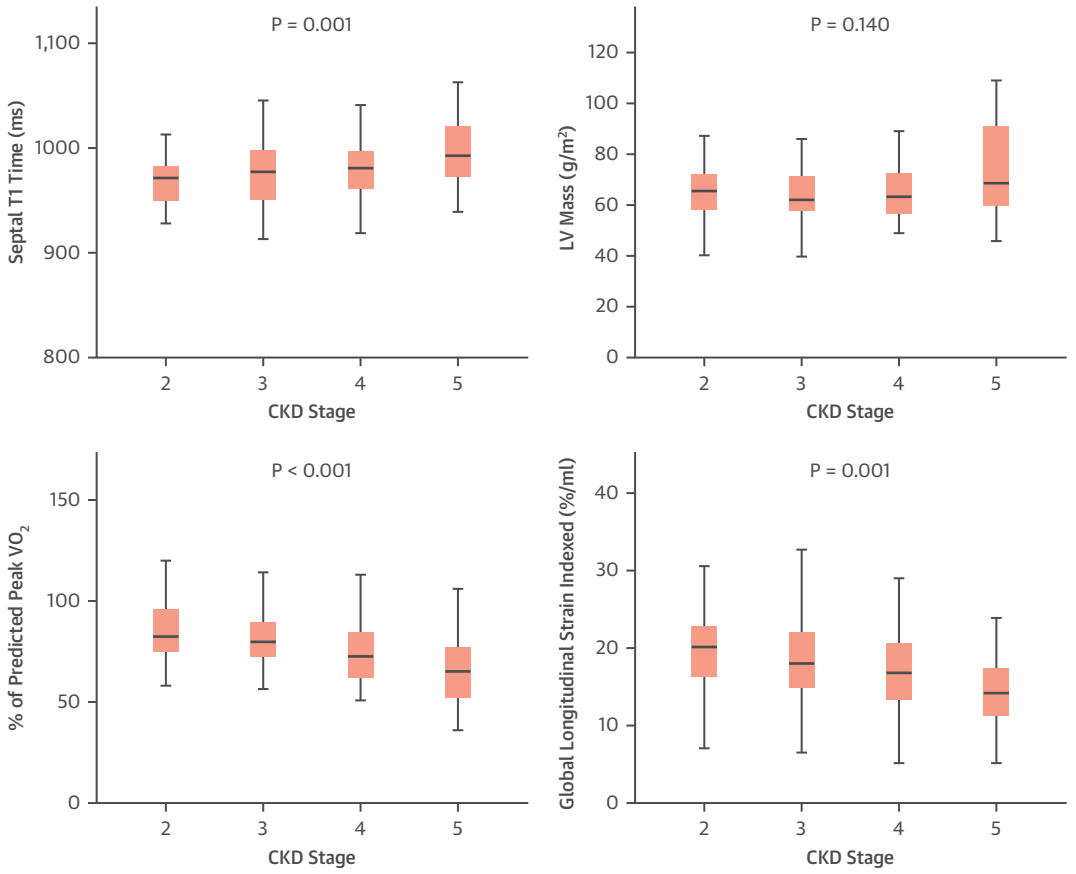

The p values are derived from the Jonckheere Terpstra test for trend. The maximum height of the whisker is 1.5 times the interquartile range.
CKD = chronic kidney disease; LV = left ventricular.

no difference in the patterns of LGE seen between the CKD stage 2 and 3 groups.

BLOOD BIOMARKERS OF MYOCARDIAL FIBROSIS AND DYSFUNCTION. There was a significant trend for serum biomarkers of heart failure (NT-proBNP: $p < 0.001$), myocardial injury (high-sensitivity troponin-T: $p < 0.001$), and myocardial fibrosis (P1NP: $p < 0.001$; P3NP: $p < 0.001$) to increase with advancing CKD stage (**Table 1, Central Illustration**). Aldosterone (test for trend: $p = 0.03$) and FGF-23 (test for trend: $p < 0.001$) also increased with worsening CKD, with no difference in alpha-Klotho levels. There was no association between native myocardial T_1 time and biomarkers of fibrosis. Native myocardial T_1 time was correlated with NT-proBNP ($r = 0.404$; $p < 0.001$) and FGF23 ($r = 0.202$; $p = 0.002$) but not with high-sensitivity troponin T. There was no association between LGE and NT-proBNP or high-sensitivity troponin T.

CARDIOPULMONARY STRESS ECHOCARDIOGRAPHY. CPESE data were available for 127 of 137 subjects (**Table 3**). Six subjects could not cycle, 2 declined the test, and 2 could not tolerate the face mask. Effort tolerance was inversely associated with worsening CKD severity as measured by several CPESE biomarkers including %predicted VO_2Peak, % predicted VO_2 at the ventilatory threshold (% predicted VO_2VT), and VE/VCO_2. Indexed myocardial GLS on resting echocardiography also reduced with worsening CKD stage ($p < 0.001$), whereas indexed LA volume and resting E/e′ increased (LA vol $p = 0.040$; Resting E/e′ $p = 0.009$) (**Figure 1**).

REGRESSION MODELS FOR PREDICTION OF NATIVE T_1. Multivariable regression modeling was

TABLE 3 Data From Cardiopulmonary Exercise Testing With Stress Echocardiography

	CKD 2 (n = 35)	CKD 3 (n = 35)	CKD 4 (n = 30)	CKD 5 (n = 27)	p Value (Trend)
Peak VO_2, ml/kg/min	24.2 ± 6.3	20.3 ± 5.2	20.0 ± 5.9	17.8 ± 5.2	**<0.001**
VO_2 at VT, ml/kg/min	14.4 ± 3.7	12.5 ± 2.9	12.5 ± 4.4	11.0 ± 3.1	**<0.001**
% predicted VO_2Peak	86 ± 17	81 ± 15	75 ± 21	65 ± 17	**<0.001**
% predicted VO_2VT	52 ± 13	51 ± 13	48 ± 19	41 ± 12	**0.001**
VE/VCO_2	26.5 ± 6.7	28.7 ± 4.6	28.9 ± 4.9	30.9 ± 10.5	**0.007**
Resting HR, beats/min	82 ± 18	88 ± 14	90 ± 23	90 ± 14	**0.045**
% predicted maximum HR	91 ± 12	93 ± 9	91 ± 10	84 ± 8	**0.002**
METS	8.2 ± 2.0	6.8 ± 1.6	6.9 ± 1.7	6.5 ± 1.5	**0.001**
RER	1.20 ± 0.08	1.21 ± 0.09	1.19 ± 0.09	1.18 ± 0.11	0.342
Borg score	17 ± 2	16 ± 2	16 ± 2	17 ± 2	0.846
LA vol index, ml/m^2	22 ± 8	22 ± 4	25 ± 11	26 ± 11	**0.040**
GLSi echo, %/ml	20.00 ± 6.00	18.90 ± 6.70	17.10 ± 5.80	13.70 ± 6.30	**0.001**
E/A ratio rest	1.10 ± 0.39	0.90 ± 0.20	1.01 ± 0.33	1.03 ± 0.36	0.431
E/A ratio exercise	1.06 ± 0.22	0.99 ± 0.21	1.06 ± 0.29	1.08 ± 0.22	0.929
Lateral e′ rest, cm/s	12.0 ± 3.1	10.0 ± 2.9	10.2 ± 3.0	10.9 ± 3.5	0.177
Lateral e′ exercise, cm/s	14.20 ± 2.71	13.10 ± 3.40	13.80 ± 3.00	15.50 ± 3.60	0.381
Lateral E/e′ rest	5.81 ± 1.46	6.56 ± 1.82	7.19 ± 2.00	7.62 ± 3.46	**0.009**
Lateral E/e′ exercise	7.08 ± 1.19	7.54 ± 2.26	7.85 ± 2.07	8.10 ± 2.20	0.992

Values are mean ± SD. The Jonckheere Terpstra test was used to assess for trend in continuous variables across the CKD stages. A p value <0.05 was considered to be statistically significant **(bold)**.

e′ = early diastolic tissue velocity measured at the level of the mitral valve annulus; E/e′ = ratio of transmitral early blood flow velocity to early diastolic tissue velocity; GLSi = global longitudinal strain on echo; HR = heart rate; LA = left atrial; METS = metabolic equivalents; RER = respiratory exchange ratio; VE/VCO_2 = ratio of minute ventilation to carbon dioxide produced; VO_2Peak = peak oxygen uptake; VO_2 VT = peak oxygen uptake at the ventilatory threshold.

performed to assess whether the association between native myocardial T_1 time and eGFR was independent of LV afterload as measured by systolic pressure and aortic distensibility. In a multivariable regression model with septal T_1 time as the dependent variable and covariates of systolic blood pressure, age, eGFR, aortic distensibility, and sex, no measure of afterload was independently associated with native T_1 time. Decreasing eGFR ($p = 0.004$) and female sex ($p = 0.039$) were the only significant independent predictors (Supplemental Tables 1 and 2).

FUNCTIONAL CORRELATES OF MYOCARDIAL FIBROSIS. CPESE and T1. On univariable analysis, no CPESE variables correlated with native myocardial T_1 time, but both % predicted VO_2Peak and % predicted VO_2VT were positively associated with myocardial GLSi on echocardiography (% predicted VO_2Peak: $r = 0.206$; $p = 0.039$; percent predicted peak oxygen carrying capacity at the ventilatory threshold [%VO_2VT]: $r = 0.325$; $p = 0.001$) and CMR (% predicted VO_2Peak: $r = 0.063$; $p = 0.491$; %VO_2VT: $r = 0.274$; $p = 0.002$). GLSi and native myocardial T_1 time were inversely correlated ($r = -0.227$; $p = 0.021$). Resting and exercise E/e′ were also associated with native myocardial T_1 time (rest: $r = 0.201$; $p = 0.028$; exercise: $r = 0.235$; $p = 0.025$).

CPESE and serum biomarkers of fibrosis. Exercise capacity (% predicted VO_2Peak and %VO_2VT) were associated with P3NP, ($r = -0.352$; $p < 0.001$; and $r = -0.233$; $p = 0.010$, respectively). P3NP was also associated with echo GLSi ($r = -0.212$; $p = 0.031$) and E/e′ (rest: $r = 0.304$; $p = 0.001$).

PREDICTORS OF EXERCISE TOLERANCE. Given the potential for multiple associations between confounding markers of exercise tolerance and factors such as LV mass, myocardial strain, fibrosis, hemoglobin, eGFR, and age, multivariable backward linear regression modeling was performed with % predicted VO_2Peak as the dependent variable. Female sex ($p = 0.003$), hemoglobin ($p = 0.012$), and LA volume ($p = 0.002$) were positive predictors of % predicted VO_2 Peak, whereas body mass index ($p = 0.011$), high-sensitivity troponin T ($p < 0.001$), and native myocardial T_1 time ($p = 0.008$) were negative predictors. This model was positive with a p value of <0.001 and it explained 56% of the variability seen.

REPRODUCIBILITY. No systemic bias was detected by Bland-Altman analysis between intraoperator and interoperator agreement for native myocardial T_1 times. The mean intraobserver and interobserver differences were −1 ± 6 ms (95% limits of agreement: −12 to 10 ms) and −1 ± 7 ms (95% limits of agreement: −13 to 11 ms), respectively.

DISCUSSION

In this cross-sectional study of subjects with pre-dialysis nondiabteic CKD who had myocardial ischemia excluded native myocardial T_1 time, a histologically validated

marker of interstitial myocardial fibrosis, had a graded inverse relationship with kidney function. The association was independent of the effects of LV afterload including hypertension, aortic distensibility, and LV hypertrophy. Serum biomarkers of fibrosis also increased, and echo-based global longitudinal strain decreased with stage of CKD. Both native myocardial T_1 on CMR and serum pro-collagen biomarkers of fibrosis were associated with surrogate markers of elevated LV end-diastolic pressure, increasing diastolic stiffness (NT-proBNP and mitral E/e′) and progressive functional limitation on cardiopulmonary exercise testing, thereby supporting the hypothesis that myocardial fibrosis contributes to impaired cardiac performance in CKD.

These data add to previous observational reports demonstrating increased native T_1 times in ESRD (7,8) and increased T_1 times and ECV in early-stage CKD (9). The prevalence of myocardial late gadolinium enhancement was low (8 of 67) in keeping with previous reports (16), and highlights the limitation of LGE imaging for detecting subtle diffuse interstitial changes, although we acknowledge the lack of histological validation of T_1 and fibrosis in CKD. Our finding that myocardial T_2 time also increased with worsening CKD and was correlated with myocardial native T_1 time suggests a possible contribution of myocardial edema, as previous reported in ESRD before and after dialysis (17). Further research is required to define the relative contributions of water and fibrosis to the elevated T_1 times in CKD. The lack of correlation between native T_1 and serum biomarkers of fibrosis suggests no single biomarker appears sufficient to characterize the myocardium comprehensively due to a heterogeneous response. This finding is similar to recent data in aortic stenosis (18), and we speculate that imaging and serum biomarkers might offer independent "signals" of myocardial fibrosis, thus requiring an integrative approach.

Functional limitation was demonstrated on cardiopulmonary exercise testing with a progressive deterioration with advancing stage of CKD. This finding is consistent with data from a large cross-sectional study demonstrating a graded reduction in VO_2Peak and peak cardiac power with worsening kidney function (19). Exercise tolerance was inversely correlated with serum biomarkers of fibrosis and echo-derived global longitudinal strain—a validated surrogate biomarker of myocardial fibrosis and a prognostic marker of outcome in CKD (20). Although causation cannot be demonstrated from our data, the results support a hypothesis that diffuse interstitial myocardial fibrosis (and possibly myocardial edema) may be drivers of myocardial dysfunction and exercise intolerance as CKD advances.

Both native myocardial T_1 times and circulating levels of P3NP have been independently correlated with histologically proven myocardial fibrosis, including in hypertensive cardiomyopathy, aortic stenosis, and idiopathic dilated cardiomyopathy (21). While histological correlation of fibrosis with native T_1 time is lacking in CKD, there is other evidence of fibrotic disease. Galectin-3, a serum biomarker of fibrosis, increases as eGFR falls, and has been associated with progressive abnormalities of GLS and all-cause mortality in CKD (8,22). Our study has demonstrated an inverse relationship between eGFR and serum biomarkers of collagen turnover as well as FGF-23, a hormone linked to development of LVH and heart failure (23).

STUDY LIMITATIONS. This was a cross-sectional study, so neither longitudinal progression nor a causal relationship between imaging/serum biomarkers and declining kidney function can be assumed. A longitudinal follow-up study would be necessary to better understand the influence of declining kidney function on the progression of variables under study and clinical outcomes but would be prolonged, difficult, and expensive to undertake. The study population was highly selected, enrolling subjects without a history of diabetes mellitus or CAD; hence, applicability to the wider CKD population is limited. The high proportion of subjects with vasculitis (17%) means that we are unable to exclude an independent influence of myocardial inflammation and scarring due to these disorders. Only a small proportion of our patients received gadolinium contrast for these research CMR studies due to guideline recommendations for use with eGFR >30 ml/min/1.73 m^2. This limited ECV measurement and detection of irreversible reparative fibrosis detected by LGE. Our study was also limited by size. The increase in native myocardial T_1 times were smaller than predicted from power calculations and below our pre-specified minimal detectable difference, as were changes in echo markers of diastolic function across stages of CKD. There was no significant difference in ECV between CKD stage 2 and 3. However, this difference may have been underestimated as the sample size was small due to the limited eligibility for gadolinium.

CONCLUSIONS

In subjects across the spectrum of nondialysis CKD without diabetes or ischemic heart disease, myocardial fibrosis assessed by native myocardial T_1 time

showed a graded inverse association with kidney function independent of the effects of LV afterload. The observed deterioration in diastolic function and effort tolerance, coupled with a rise in validated biomarkers of fibrosis, heart failure, and myocardial injury, are consistent with a role for myocardial fibrosis as an early and key intermediary in the development of uremic cardiomyopathy. Noninvasive and noncontrast-based myocardial characterization with CMR T_1 mapping is robust and might allow better risk stratification of myocardial disease and potentially targeted antifibrotic therapy.

ACKNOWLEDGMENT The authors would like to thank Mr. James Hodson for his help with statistics.

AUTHOR RELATIONSHIP WITH INDUSTRY

This study is supported by the British Heart Foundation (PG/15/117/31961). Dr. Weston is funded by the National Institute for Health Research (NIHR) Birmingham Biomedical Research Centre at the University Hospitals Birmingham NHS Foundation Trust and the University of Birmingham. All other authors have reported that they have no relationships relevant to the contents of this paper. This paper presents independent research supported by the NIHR Birmingham Biomedical Research Centre at the University Hospitals Birmingham NHS Foundation Trust and the University of Birmingham. The views expressed are those of the author(s) and not necessarily those of the NHS, the NIHR, or the Department of Health and Social Care.

ADDRESS FOR CORRESPONDENCE: Dr. Nicola Edwards, Department of Cardiology, Green Lane Cardiovascular Service, Auckland City Hospital, 2 Park Road, Grafton, Auckland 1023, New Zealand. E-mail: NicolaEd@adhb.govt.nz.

PERSPECTIVES

COMPETENCY IN MEDICAL KNOWLEDGE 1: Heart failure and sudden death rates are the primary cause of death in advanced renal disease, and risk increases as glomerular filtration declines.

COMPETENCY IN MEDICAL KNOWLEDGE 2: Myocardial fibrosis has been detected on cardiac biopsies in patients with end-stage renal disease and is postulated to contribute to uremic cardiomyopathy. This finding has been supported by the surrogate marker of high native T_1 myocardial times on CMR T_1 mapping techniques and abnormalities of deformation on echo. The functional impact of this finding is not known.

COMPETENCY IN PATIENT CARE AND PROCEDURAL SKILLS: Diffuse interstitial myocardial fibrosis assessed by CMR and blood biomarkers increases with stage of CKD and is associated with deleterious changes in the heart and exercise tolerance.

TRANSLATIONAL OUTLOOK 1: Myocardial fibrosis might be a target for pharmacological treatments in CKD.

TRANSLATIONAL OUTLOOK 2: Treatments to reduce myocardial disease in CKD might reduce the disproportionate cardiovascular event rate.

REFERENCES

1. Matsushita K, van der Velde M, Astor BC, et al. Association of estimated glomerular filtration rate and albuminuria with all-cause and cardiovascular mortality in general population cohorts: a collaborative meta-analysis. Lancet 2010;375:2073–81.

2. Couser WG, Remuzzi G, Mendis S, Tonelli M. The contribution of chronic kidney disease to the global burden of major noncommunicable diseases. Kidney Int 2011;80:1258–70.

3. Wanner C, Amann K, Shoji T. The heart and vascular system in dialysis. Lancet 2016;388:276–84.

4. Edwards NC, Moody WE, Chue CD, Ferro CJ, Townend JN, Steeds RP. Defining the natural history of uremic cardiomyopathy in chronic kidney disease: the role of cardiovascular magnetic resonance. J Am Coll Cardiol Img 2014;7:703–14.

5. Mark PB, Johnston N, Groenning BA, et al. Redefinition of uremic cardiomyopathy by contrast-enhanced cardiac magnetic resonance imaging. Kidney Int 2006;69:1839–45.

6. Hensen LCR, Goossens K, Delgado V, Rotmans JI, Jukema JW, Bax JJ. Prognostic implications of left ventricular global longitudinal strain in predialysis and dialysis patients. Am J Cardiol 2017;120:500–4.

7. Graham-Brown MP, March DS, Churchward DR, et al. Novel cardiac nuclear magnetic resonance method for noninvasive assessment of myocardial fibrosis in hemodialysis patients. Kidney Int 2016;90:835–44.

8. Rutherford E, Talle MA, Mangion K, et al. Defining myocardial tissue abnormalities in end-stage renal failure with cardiac magnetic resonance imaging using native T1 mapping. Kidney Int 2016;90:845–52.

9. Edwards NC, Moody WE, Yuan M, et al. Diffuse interstitial fibrosis and myocardial dysfunction in early chronic kidney disease. Am J Cardiol 2015;115:1311–7.

10. Messroghli DR, Moon JC, Ferreira VM, et al. Clinical recommendations for cardiovascular magnetic resonance mapping of T1, T2, T2* and extracellular volume: A consensus statement by the Society for Cardiovascular Magnetic Resonance (SCMR) endorsed by the European Association for Cardiovascular Imaging (EACVI). J Cardiovasc Magn Reson 2017;19:75.

11. Liu B, Dardeer AM, Moody WE, et al. Reference ranges for three-dimensional feature tracking cardiac magnetic resonance: comparison with two-dimensional methodology and relevance of age and gender. Int J Cardiovasc Imaging 2018;34:761–75.

12. Captur G, Gatehouse P, Keenan KE, et al. A medical device-grade T1 and ECV phantom for global T1 mapping quality assurance-the T1 Mapping and ECV Standardization in cardiovascular magnetic resonance (T1MES) program. J Cardiovasc Magn Reson 2016;18:58.

13. Jones NL, Makrides L, Hitchcock C, Chypchar T, McCartney N. Normal standards for an incremental progressive cycle ergometer test. Am Rev Respir Dis 1985;131:700–8.

14. Balady GJ, Arena R, Sietsema K, et al. Clinician's guide to cardiopulmonary exercise testing in adults: a scientific statement from the American Heart Association. Circulation 2010;122:191–225.

15. Hayer MK, Edwards NC, Slinn G, et al. A randomized, multicenter, open-label, blinded end point trial comparing the effects of spironolactone to chlorthalidone on left ventricular mass in patients with early-stage chronic kidney disease: Rationale and design of the SPIRO-CKD trial. Am Heart J 2017;191:37–46.

16. Price AM, Hayer MK, Vijapurapu R, et al. Myocardial characterization in pre-dialysis chronic kidney disease: a study of prevalence, patterns and outcomes. BMC Cardiovasc Disord 2019;19:295.

17. Hayer MK, Radhakrishnan A, Price AM, et al. Early effects of kidney transplantation on the heart—a cardiac magnetic resonance multiparametric study. Int J Cardiol 2019;293:272–7.

18. Treibel TA, Lopez B, Gonzalez A, et al. Reappraising myocardial fibrosis in severe aortic stenosis: an invasive and non-invasive study in 133 patients. Eur Heart J 2018;39:699–709.

19. Ting SM, Iqbal H, Kanji H, et al. Functional cardiovascular reserve predicts survival pre-kidney and post-kidney transplantation. J Am Soc Nephrol 2014;25:187–95.

20. Rakhit DJ, Zhang XH, Leano R, Armstrong KA, Isbel NM, Marwick TH. Prognostic role of subclinical left ventricular abnormalities and impact of transplantation in chronic kidney disease. Am Heart J 2007;153:656–64.

21. Lopez B, Gonzalez A, Ravassa S, et al. Circulating biomarkers of myocardial fibrosis: the need for a reappraisal. J Am Coll Cardiol 2015;65:2449–56.

22. Tuegel C, Katz R, Alam M, et al. GDF-15, Galectin 3, soluble ST2, and risk of mortality and cardiovascular events in CKD. Am J Kidney Dis 2018;72:519–28.

23. Grabner A, Schramm K, Silswal N, et al. FGF23/FGFR4-mediated left ventricular hypertrophy is reversible. Sci Rep 2017;7:1993.

KEY WORDS myocardial fibrosis, T_1 mapping, uremic cardiomyopathy

APPENDIX For supplemental tables, please see the online version of this paper.

Go to http://www.acc.org/jacc-journals-cme to take the CME/MOC/ECME quiz for this article.